Design and Fabrication of Heat Transfer Surfaces from Superplastic Material

Abstract: The production of complex heat transfer surfaces (i.e., those without straight fins) is restricted by available fabrication techniques, materials, geometries, and cost. Based on the superplastic sheet thermoforming process, a new technique for fabricating these complex surfaces by a relatively simple, low cost process has been developed. The resulting surfaces have excellent heat transfer characteristics and can be used in a wide variety of applications. Surface design is discussed, and heat transfer and flow friction test data on various surface patterns are presented. The application of these results to unique design situations is demonstrated and particular examples are discussed.

Introduction

The dissipation of waste heat is a problem in many industries today, including the electronics industry. More efficient and low cost techniques for removing thermal energy from a source and transporting it to a sink are constantly being developed. The finned surface is well known as a heat transfer medium. When a fin is disrupted or serpentined, turbulence is introduced into the fluid passing over the surface and heat transfer is enhanced. However, flow friction (fluid power loss) is also an important consideration, particularly concerning low density fluids such as air, since heat transfer gains made by turbulation may be offset by friction losses. The design and development process should maximize heat transfer and minimize friction losses, although the complex heat transfer surface that meets these requirements may be expensive and difficult to fabricate.

Kays and London [1] describe a high performance surface as one which has a basic characteristic of high heat flux relative to friction power expenditure. A surface fabricated from sheet stock into a pattern with a high fin density can be designed to produce this characteristic. Factors that affect the design are the hydraulic diameter of the individual flow passages and any geometric modification of the passages that promotes disruption of the fluid boundary layer.

Because of available materials and fabrication techniques, the designer does not always have the option of

choosing the best surface pattern. To reduce product cost, he must very often choose a heat transfer design which adds unduly to the bulk and weight of the product, fluids must be supplied at higher Reynolds numbers, and ventilation ports that can cause safety, aesthetic, or other problems must be added.

The superplastic sheet thermoforming process provides an inexpensive and relatively simple method of fabricating complex surfaces. With this process, sheet material is formed by air pressure in a single heated die. A sample die and two pieces formed in a complex surface pattern are shown in Fig. 1. Forming parameters are relatively moderate.

The material used in this investigation was a 78 percent zinc, 22 percent aluminum alloy with a thermal conductivity of 85 BTU/hr-ft-°F. A comprehensive view of superplasticity from metallurgy through design and applications data is given by Refs. [4] through [9].

Even if complex finned surfaces are available on a cost-competitive basis, how does one obtain design information for specific geometries? Complex surfaces defy a strictly analytical approach and, therefore, reliance must be placed on empirical data. This paper describes the development, from classical compact heat exchanger design theory, of a generalized procedure for the analysis and design of various heat transfer devices employing complex finned surfaces.

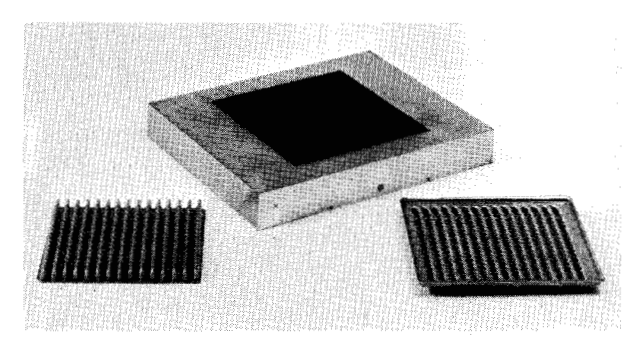


Figure 1 Sample die and two parts, showing complex pattern.

Various surfaces have been fabricated and tested, and the results are presented in the form of basic heat transfer and flow friction characteristics. The test procedure and method of data resolution have been derived from the work of Kays, London and Ferguson [1-3]. Specific surface patterns have been designed not only to test heat transfer parameters but also to demonstrate the capabilities of the superplastic sheet thermoforming process in this application.

The application of the basic surface characteristics to various design situations is discussed. Electronic cooling applications are emphasized, although this work is generally applicable to a wide variety of situations. (The original work by Kays and London was first applied to the design of compact heat exchangers for gas turbine regenerators.)

Nomenclature

- A Total heat transfer area on one side of exchanger
- A_f Minimum free flow area of exchanger
- $A_{\rm F}$ Total fin area on one side of exchanger
- A_w Area for heat transfer across flow separator sheets
- C Fluid stream capacity rate (mass flow $\times C_P$)
- $C_{\rm P}$ Fluid specific heat at constant pressure
- D_h Hydraulic diameter
- F Function of ()
- f Mean friction factor defined on the basis of mean surface shear stress
- G Flow-stream mass velocity (mass flow/area) on one side of exchanger
- g_c Proportionality factor in Newton's second law
- h Unit conductance for thermal-convection heat transfer
- K_c Contraction loss coefficient for flow at heat exchanger entrance
- $K_{\rm e}$ Expansion loss coefficient for flow at exchanger exit
- K Unit thermal conductivity

- L Total heat exchanger flow length
- m Fin effectiveness parameter
- P Pressure
- q Heat transfer rate
- Re Reynolds number $(\rho V D_h/\mu)$
- STN Stanton number (h/GC_P)
- T Temperature
- U Unit overall thermal conductance
- V Fluid stream mean velocity
- v Specific volume
- ΔX Flow separator sheet thickness
- Δ Difference or increment
- δ Fin thickness
- η Total surface temperature effectiveness due to the addition of fins
- λ Effective fin length
- μ Viscosity coefficient
- ρ Density
- σ Ratio of free flow area to frontal area of exchanger

Subscripts:

- c Cold side of test sample
- h Hot side of test sample
- m Mean value
- l Before test sample
- 2 After test sample
- in A mixed mean value of the property into one side of the device
- out A mixed mean value of the property out of one side of the device
- a,b Different functions (F) of same independent variable

Surface design

In cooling electronics, as in other applications, the ultimate heat sink is air. With standard blower hardware, air can be supplied in relatively high volumes at low pressure resistances. However, the space and cost allotted to heat transfer devices are usually at a premium, and other design factors, such as acoustic noise, may also be directly related to air flow. Considering these factors, it is essential that heat transfer devices be compact, and low cost, while providing high performance. In many cases, this eliminates the straight fin, or two-dimensional design, which is available with extrusion techniques.

One compact, high performance pattern that is easily reproducible by the superplastic sheet thermoforming process is the serpentine corrugate pattern shown in Figs. 2 through 5. This type of pattern will produce a momentum vector perpendicular to the flow direction of the main fluid stream, creating turbulence in the flow, even in the lower range of Reynolds numbers where flow is normally considered laminar. At moderate and higher Reynolds numbers, premature transition to turbu-

lent flow can be induced, and in some cases actual boundary layer separation may occur. It is well established that greater degrees of momentum exchange within a fluid, as encountered in a turbulent flow situation, will enhance heat transfer. In fact, a review of the literature shows an excellent performance potential for the serpentine corrugate pattern [1,3].

Among the many requirements of the design for a specific application, the primary consideration is to maximize heat flux relative to the expenditure of power in fluid friction. To achieve this, the designer must consider specific geometric parameters such as the amplitude of the wave, the number of waves per inch, the fin length, the hydraulic diameter, etc.

Since this type of surface defies a strictly analytical approach, it was decided to fabricate and test samples of various surfaces to generate the necessary data. The test procedure was derived from work by Kays and London on compact heat exchangers. Layers of the material were fabricated into small, symmetrical, 90-degree crossflow heat exchangers. A diagram of the flow test facility and equipment is shown in Fig. 6. Heated air was passed through one side of the exchanger and room temperature air through the other side; air temperatures at the entrance and exit points could be measured to obtain mixed mean temperature differences across the exchanger. Flow rates were varied on both sides, and the corresponding temperatures and flow rates were recorded.

To be applied to a heat transfer design situation, the data must be reduced to a form of nondimensional heat transfer and flow friction characteristic that is a function of the fluid stream properties and the specific geometry. Since air at moderate temperatures and velocities was the test fluid, it was decided to present the data by means of the following nondimensional relationships:

$$STN$$
 (Stanton number) = $\frac{h}{GC_P} = F_a (Re)$

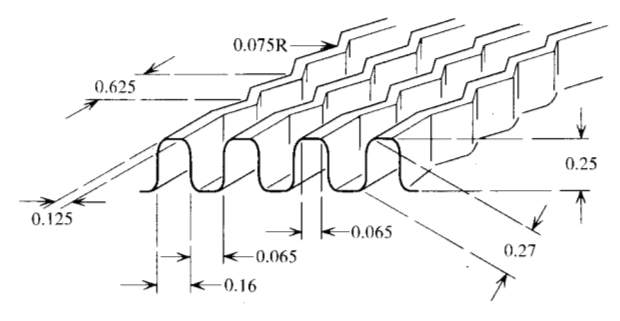
and

f (friction factor) = F_b (Re),

where

$$Re ext{ (Reynolds number)} = \frac{\rho V D_h}{\mu}.$$

Since the geometry in all flow passages of a given sample may not be the same, hydraulic diameter is defined as four times the mean cross-sectional area divided by mean perimeter, and flow velocity is based on minimum free flow area. Note that the Stanton number and friction factor are also functions of specific surface geometry, material properties, and fabrication-dependent properties such as the thermal contact resistance of the inter-



 $D_h = 0.0129$ ft; $L/D_h = 99$; dimensions in inches

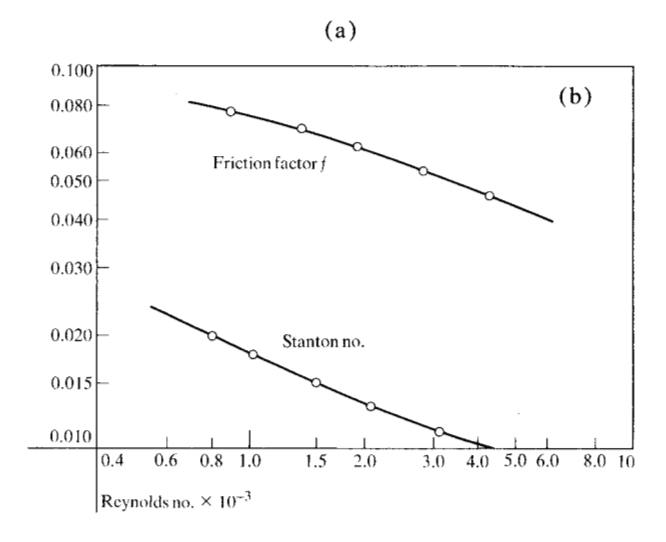


Figure 2 (a) Dimensions (in inches) and (b) Stanton number and friction factor vs Reynolds number for Pattern I (fin thickness 0.007 in.).

face joint between layers of the exchanger. However, the test units were bonded by a tin reflow process and microscopic examination revealed an excellent metallic bond at the interface joint; contact resistance was therefore not considered in converting the raw data.

There are two approaches to compact heat exchanger design, the log mean temperature difference method [10,11] and the "effectiveness-number of transfer units" (NTU) method. The NTU approach is preferred because it is less complex and has been found to yield excellent results. The utility of the NTU approach will become more apparent as it is used here to develop generalized heat transfer data not only for heat exchanger design but for a variety of design situations.

Two nondimensional groupings used in the NTU approach are defined as

1. the number of exchanger heat transfer units (NTU):

$$NTU = \frac{UA}{C}$$
, and (1)

2. the exchanger temperature effectiveness:

$$E_{\rm h} = \frac{T_{\rm h,in} - T_{\rm h,out}}{T_{\rm h,in} - T_{\rm c,in}};$$
 (2)

$$E_{\rm c} = \frac{T_{\rm c,out} - T_{\rm c,in}}{T_{\rm h,in} - T_{\rm c,in}}.$$
 (3)

To begin the development, there are three basic differential equations that describe the energy exchange between the fluid streams of the heat exchanger. The equation for heat transfer between hot and cold fluid streams across the exchanger is:

$$\frac{dq}{dA} = U \left(T_{\rm h} - T_{\rm c} \right),\tag{4}$$

where U (overall conductance for heat transfer) is determined by

$$\frac{1}{U_{\rm h}} = \frac{1}{h_{\rm h}\eta_{\rm h}} + \frac{\Delta X}{K(A_{\rm w}/A_{\rm h})} + \frac{1}{h_{\rm c}\eta_{\rm c}(A_{\rm c}/A_{\rm h})}$$
(5)

The steady-state heat transfer rate through a surface element of area dA and the effect on the two fluid streams as they pass through the exchanger are given by two rate equations:

$$\frac{dq}{dA} = \frac{C_{\rm c} dT}{L dL} \bigg|_{\rm c}; \tag{6}$$

$$\frac{dq}{dA} = \frac{C_{\rm h} dT}{L dL} \bigg|_{\rm h},\tag{7}$$

where L (the dimension of the exchanger in the flow direction) is defined for simplicity as the same on both hot and cold sides.

Equation (5) should be explained further. A similar expression for U_c can be stated, and since the exchanger test samples were arbitrarily assembled such that the area for heat transfer was the same on both the hot and cold sides, then

$$U_{\rm h} = U_{\rm c} = U \tag{8}$$

Also, the convective conductances in Eq. (5) are modified by an expression from fin theory,

$$\eta = 1 - \frac{A_{\rm F}}{A} \left(\frac{1 - \tanh m\lambda}{m\lambda} \right),\tag{9}$$

where

$$m = (2h/K\delta)^{\frac{1}{2}} \tag{10}$$

By solving Eqs. (4), (6) and (7), a relationship can be derived for U (conductance) as a function of effectiveness, the mass flows through both sides, and the flow orientation. In the case of 90-degree crossflow, this relationship cannot be expressed in a closed form. However, Eqs. (4), (6) and (7) have been solved by Mason [12] with the solution expressed in a series form.

According to Mason, the solution can be expressed in the following form:

$$E_{\rm h} = (NTU)_{\rm h}\phi; \tag{11}$$

$$E_{c} = (NTU)_{c}\phi, \tag{12}$$

where

$$\phi = [(NTU)_{h} (NTU)_{c}]^{-1} \times \sum_{n=0}^{\infty} R_{n} (NTU)_{h} R_{n} (NTU)_{c}$$
(13)

and

$$R_{\rm n} (NTU) = 1 - \exp(-NTU) \sum_{k=0}^{n} [(NTU)^{k}/k!].$$
 (14)

For convenience and accuracy, due to the inclusion of experimental parameters measured in both the hot and cold fluid streams, Eqs. (11) and (12) are combined as follows:

$$E_{\rm h}E_{\rm c} - (NTU)_{\rm h}(NTU)_{\rm c}\phi^2 = 0,$$
 (15)

۸r

$$E_{\rm h}E_{\rm c} - \left(\frac{U_{\rm h}A}{C_{\rm h}}\right)\left(\frac{U_{\rm c}A}{C_{\rm c}}\right)\phi^2 = 0. \tag{16}$$

Therefore, if E_h , E_c , C_h and C_c are known from experimental data, Eq. (16) can be solved for U on a computer by an interval search or some similar numerical technique. Equation (5) can then be solved for h when the mass flow is the same through both sides of the exchanger and property changes due to the temperature difference are neglected. If

$$C_{\rm h} = C_{\rm c}$$

then

$$h_{\rm h} = h_{\rm c}.\tag{17}$$

By solving Eq. (16) numerically at the experimental condition expressed in Eq. (17), the Stanton number as a function of the Reynolds number for a given surface pattern can be expressed.

The other necessary design parameter is the flow friction over a given surface. Kays and London [1,2] give the following relationship for pressure drop ΔP as compared to initial pressure P_1 :

$$\frac{\Delta P}{P_1} = \frac{G^2 v_1}{2g_c P_1} \left[(K_c + 1 - \sigma^2) + 2 \left(\frac{v_2}{v_1} - 1 \right) + f \frac{A}{A_t} \frac{v_m}{v_1} - (1 - \sigma^2 - K_e) \frac{v_2}{v_1} \right],$$
(18)

Where the four terms within the brackets correspond, respectively, to the entrance effect, the flow acceleration, the core friction, and the exit effect.

For air flowing at moderate Reynolds numbers with a relatively large ratio of flow length to hydraulic diameter (L/D_h) , the core friction term is dominant, and variations in density can be neglected [2]. However, entrance and exit effects should be considered. Thus,

$$\Delta P = \frac{G^2 v_{\rm m}}{2g_{\rm c}} \left(f \frac{A}{A_{\rm f}} + K_{\rm c} + K_{\rm e} \right), \tag{19}$$

where K_c and K_e are entrance and exit coefficients. Further information on entrance and exit effects is given in Refs.[1] and [2].

If mass flow and pressure drop are known from experiment, Eq. (19) can be solved for f (friction factor) for a given geometry.

Four individual surface patterns were tested and the experimental data resolved in the manner described above. The results in the form of f and STN versus Re are shown in Figs. 2 through 5. Also shown are the dimensions of each surface. Note that two sets of curves are shown in Figs. 3 and 5. In these cases, material of two basic stock thicknesses, 0.015 and 0.030 in., was formed by the superplastic process on the same tool. The dimensional characteristics of the surfaces show some rather subtle changes in fin length and hydraulic diameter, and the consequences are apparent on the performance curves.

As previously mentioned, an assumption of constant properties was made in resolving the data and is generally made in the section below on applications. This, of course, is a simplifying assumption that may in some applications introduce significant error. For the data shown in Figs. 2 through 5 the maximum temperature difference between hot and cold sides during the experiments was less than 60°F and the maximum temperature difference encountered when computing mixed mean temperatures on one side was 26°F. In the authors' experience these temperature differences are not great enough to introduce any significant errors, but the designer should nevertheless treat each design situation as unique, at least in the initial analysis, and be aware of all simplifying assumptions. For an analysis of the effects of temperature-dependent properties, consider Ref. [13] and its bibliography.

Comparison of the data in Figs. 2 through 5 shows that differences are often quite small and trends are difficult to determine. Some conclusions, however, can be drawn. For example, surfaces with a low amplitude and a high-frequency wave pattern appear to cause less flow friction but not necessarily a lower heat transfer characteristic. This could be an important factor in electronics cooling applications where Reynolds numbers should be maintained below 2000. The friction characteristic in this Reynolds number range can greatly affect the cost and size of air moving devices required.

	Pattern IIA: $D_h = 0.0126 \text{ ft}; L/D_h = 33.8;$ dimensions in inches	Pattern IIB: $D_h = 0.0122 \text{ ft}; L/D_h = 35;$ dimensions in inches
Α	0.160	0.150
В	0.070	0.045
C	0.060	0.055
D	0.27	0.28
E	0.225	0.265

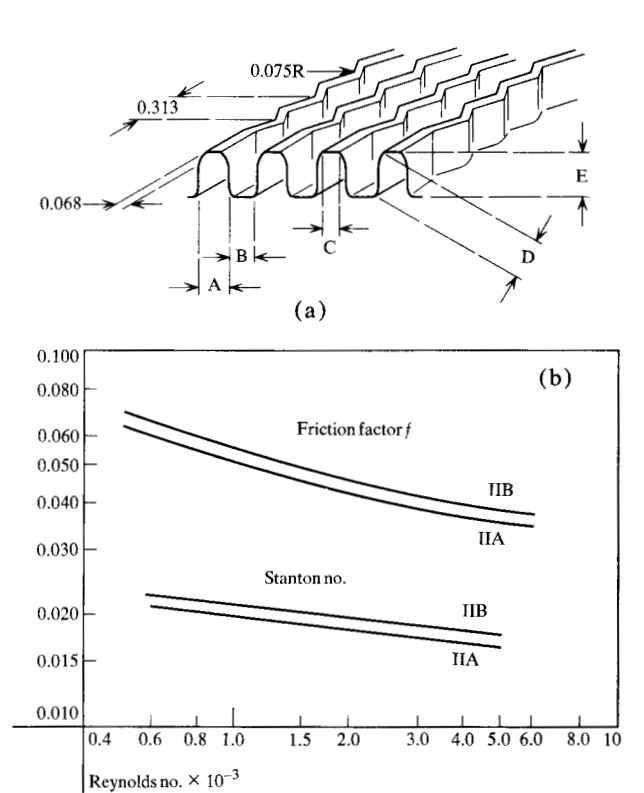
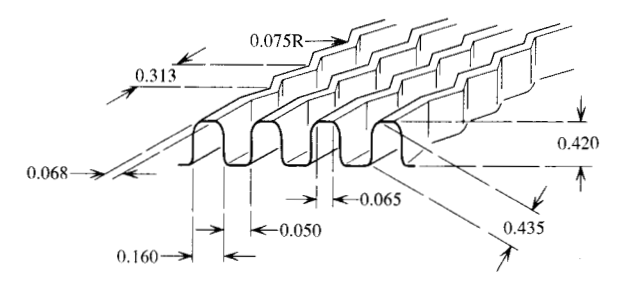


Figure 3 (a) Dimensions (in inches) for Patterns IIA and B; (b) Stanton number and friction factor vs Reynolds number for Patterns IIA and B (fin thickness 0.007 in., Pattern IIA; 0.015 in., Pattern IIB).

Note that the friction factor curve in Fig. 2 is significantly higher than those in Figs. 3 through 5. Without further study and experimentation, the exact cause of this condition cannot be determined, although it leads to some interesting observations. Note from the Figures that pattern I has a much larger wave amplitude and lower frequency than the other patterns. The hydraulic diameters, however, are very similar. This allows a relatively wide straight line or line-of-sight flow path through the patterns in Figs. 3 through 5. This is not the case in pattern I, where the entire mass of fluid must follow the wave pattern as it moves through a flow passage, whereas with the other patterns the flow passage resembles a straight pipe with a rough wall. It is therefore probable that two entirely different flow situations are represented. Regardless of the phenomena actually present, how-



 $D_{\rm h} = 0.01465 \, \text{ft}; L/D_{\rm h} = 29.1; \text{ dimensions in inches}$

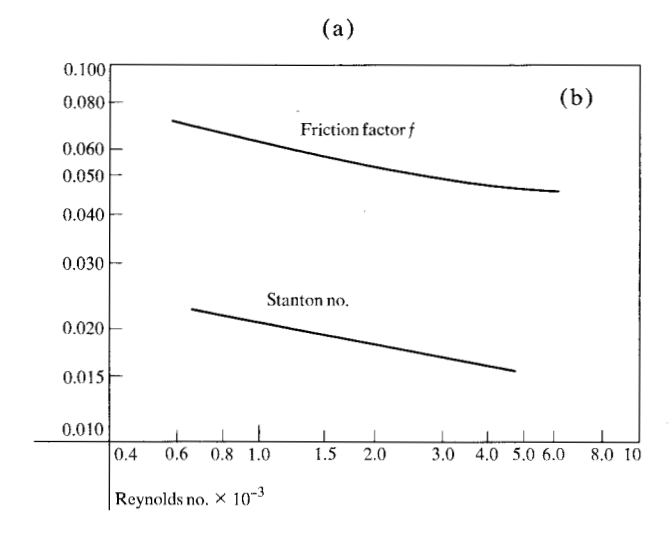


Figure 4 (a) Dimensions and (b) Stanton number and friction factor vs Reynolds number for Pattern III (fin thickness 0.010 in.).

ever, it is quite apparent that the patterns in Figs. 3 through 5 are much more advantageous for heat transfer design.

Applications

The heat transfer data in Figs. 2 through 5 can be applied to a specific design situation through the use of an equation such as

$$\frac{dq}{dA} = h(T_1 - T_2),\tag{20}$$

where T_1 is the temperature of a solid surface and T_2 the temperature of a fluid flowing past the surface. Note that to apply Eq. (20), the surface temperature distribution and the free-stream fluid temperature must be known. The free-stream fluid temperature must be carefully determined, since it is often assumed constant in so-called open-channel flow even though it varies greatly with boundary layer effects in closed-channel flow. Even with open-channel flow, one must evaluate the specific design situation carefully to determine whether the free-stream temperature is constant.

	Pattern IVA: $D_h = 0.0137 \text{ ft}; L/D_h = 26.9;$ dimensions in inches	Pattern IVB: $D_h = 0.0130 \text{ ft}; L/D_h = 28.4;$ dimensions in inches
Α	0.130	0.125
В	0.115	0.11
C	0.045	0.045
D	0.285	0.30
Е	0.265	0.28

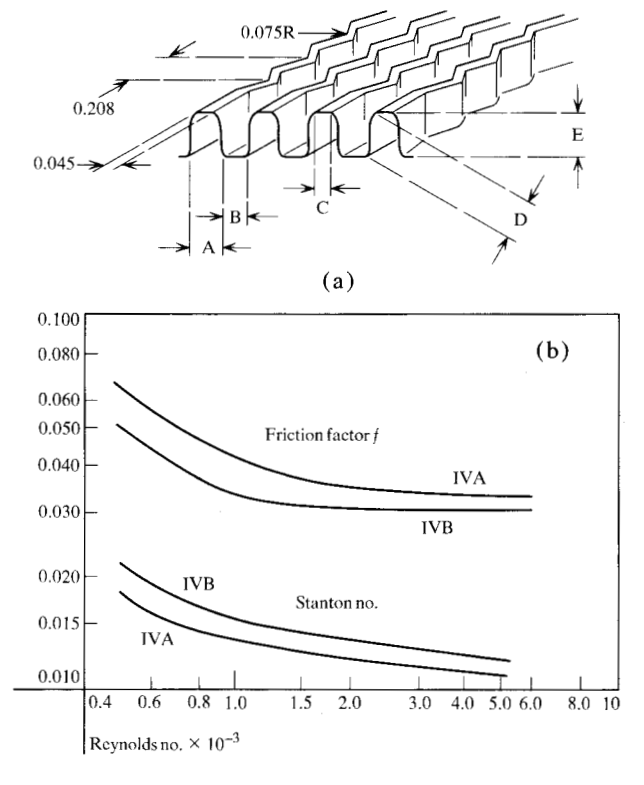


Figure 5 (a) Dimensions for Patterns IVA and B; (b) Stanton number and friction factor vs Reynolds number for Patterns IVA and B (fin thickness 0.007 in., Pattern IVA; 0.015 in., Pattern IVB).

The first application considered is the case for which a condensing fluid is present on one side of the surface with air in forced convection on the other side. At moderate and higher Reynolds numbers, this can generally be considered open-channel flow with a constant free-stream temperature. By neglecting the small losses due to conduction through the surface and a thin film of condensed liquid, the surface temperature may also be assumed constant.

This design situation arises with the device shown in Fig. 7, which is a boiling heat transfer device for cooling high power-density electronic components. The device is sealed with a vacuum over the liquid. The power input boils the liquid, which is then condensed in the fin region and reflows by gravity to the liquid pool.

For analysis of this device, a straightforward integration of Eq. (20) yields

$$q = Ah(\Delta T). \tag{21}$$

Since the temperature loss due to bubble formation and ebullition (depending on the boiling regime) can be found from boiling heat transfer theory, it is possible to completely describe the working device through Eq. (21) if the saturation vapor-pressure curve is known for the working fluid.

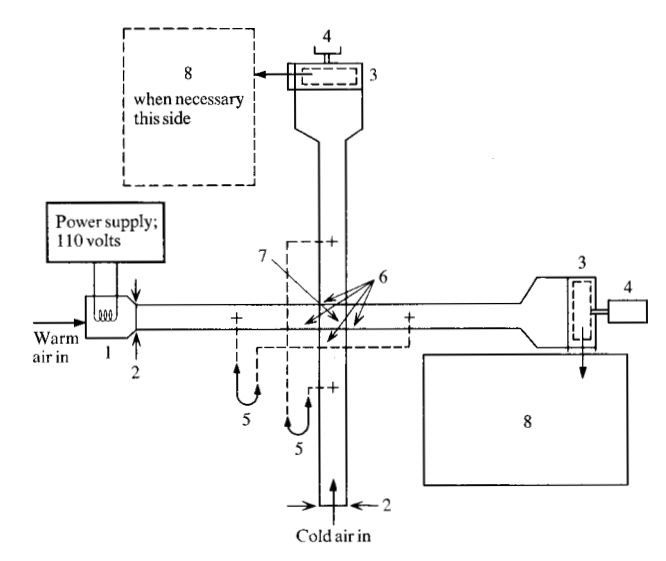
The finned surface in Fig. 7 can be made in one piece with the superplastic forming process, thereby leaving only one flange to be joined in assembling the device. This offers many advantages in cost savings and device reliability, since a hermetic seal is necessary in this application.

Another application is the finned surface bonded to a solid conducting base, of which the transistor heat sinks shown in Fig. 8 are an example. In this case, heat from a localized source is conducted through a solid substrate to the fin material and dissipated by forced convection. If the flow length over the sink is relatively small and the Reynolds numbers relatively high, the free-stream fluid temperature may be considered constant as a good approximation. However, this still leaves the complex problem of defining the temperature distribution over the solid surface. If the substrate operates at a constant heat rate or constant temperature, Eqs. (9) and (10) (derived from fin theory), can be applied with Eq. (21). In the case of the transistor heat sink the temperature distribution of the substrate is more complex, but it can be determined by a solution combining fin theory with the model for conduction in a flat plate from a heat source.

Since heat sinks are small, low cost items, it is usually most convenient to model and test the specific design. The data are commonly presented as a plot of heat sink thermal resistance (°C/W) vs air flow velocity at standard conditions. Figure 9 shows a performance curve for blackened heat sinks similar to those shown in Fig. 8. The heat sinks, made from patterns IIB and III (refer to Figs. 3 and 4), were tin-reflow-bonded to a substrate.

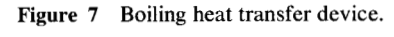
For comparison, the performance curve of an extruded aluminum sink, which is similar in size and geometry to the sink in Fig. 8 and was tested under identical conditions, is also shown in Fig. 9.

As a final application consider one obvious closedchannel flow situation in which two fluid streams flow at 90 degrees to one another as in the crossflow air-to-air heat exchanger. Considerable information on heat exchanger design for many fluid stream orientations is available [1]. For 90-degree crossflow, the design procedure is practically the reverse of that used to develop the design data. A design usually specifies the physical size, temperature limits, heat load and, perhaps, the



- Resistance heater bank
- Air flow regulators (side gate)
 Torin FE 623 blower wheels and housings
- 1/3 hp, 3450 rpm motor
- Static pressure taps and manometers
- Thermocouple measurement points
- Heat exchanger test sample
- Air flow test chamber for volume flow measurements on both sides

Figure 6 Diagram of flow test facility.



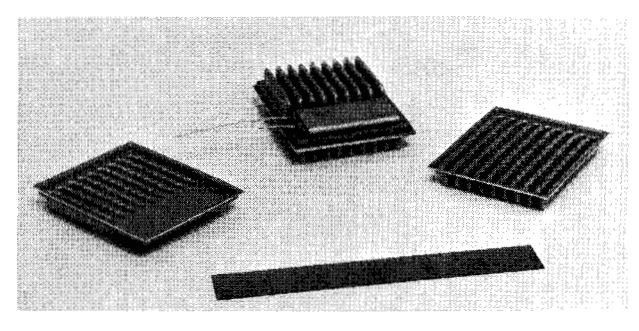
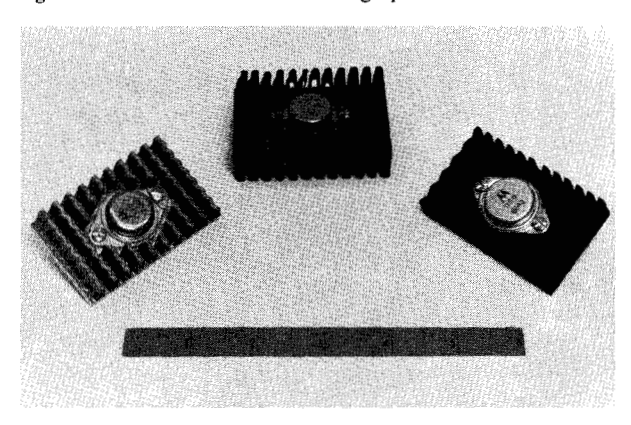


Figure 8 Heat sink elements for high-power transistors.



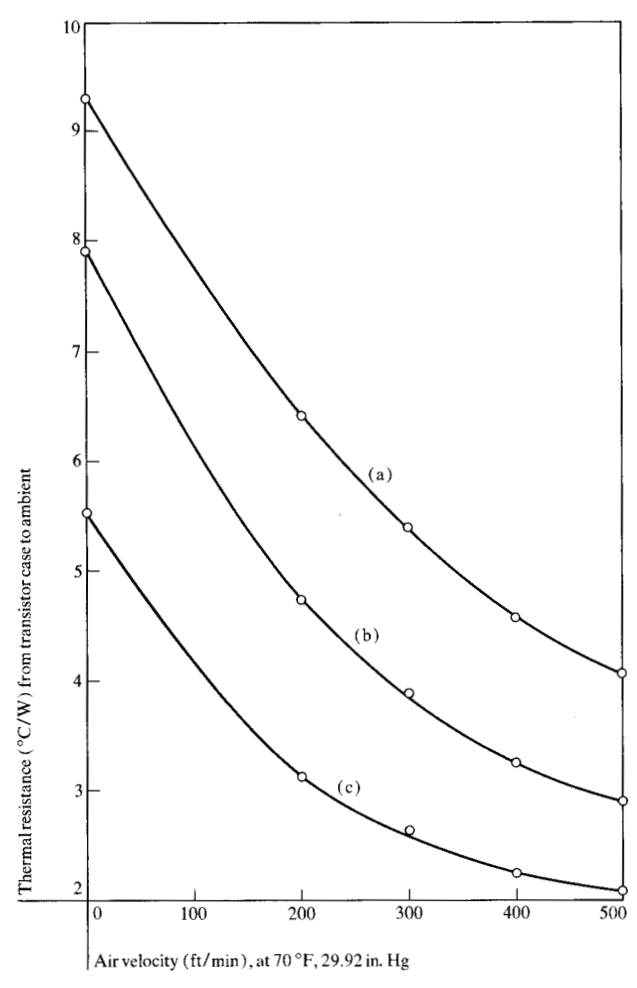


Figure 9 Performance curves for experimental transistor heat sinks similar to those of Fig. 8. (a) Extruded aluminum pattern on one side of substrate; (b) Zn-Al Pattern IIB on one side of substrate; (c) Zn-Al Pattern III on both sides of substrate.

maximum air flow limit for the exchanger. The design then becomes an iterative procedure:

- 1. A likely surface pattern is chosen.
- Reynolds numbers and thereby flow capacities and NTU values are determined for both sides of the exchanger from the appropriate design curves and surface geometry.
- 3. Overall conductance is used in place of convective conductance in Eqs. (11) and (12), but they are otherwise just integrated forms of Eq. (20). The latter equation can thus be solved for temperature effectiveness E, and the heat load to be dissipated is then determined from

$$q = C(T_{\text{out}} - T_{\text{in}}) \tag{22}$$

for both the hot and the cold sides of the exchanger.

4. Equation (19) is solved for pressure loss in the fluid passing through the exchanger.

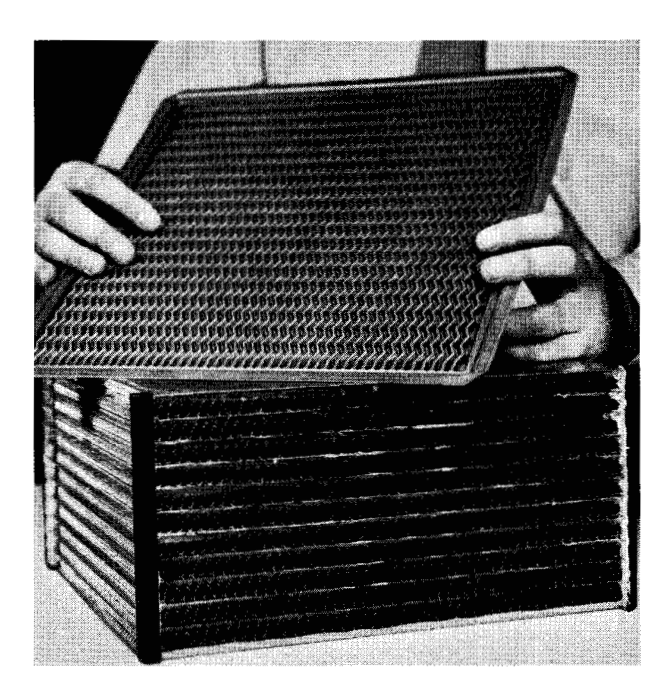


Figure 10 System/7 heat exchanger core and sample heat transfer plate.

5. If the results of step 3 or step 4 are unsatisfactory, an input quantity such as one of the Reynolds numbers, the surface geometry, or the exchanger size must be varied and the process repeated until a satisfactory design has evolved.

Figure 10 shows the core of a heat exchanger used in an air isolation unit that provides environmental protection for the IBM System/7, a process control computer. The bonding technique in this unit is a tin plating and reflow process. The use in this application of the superplastic sheet thermoforming process and the design procedure just described has resulted in a compact, high performance unit at a fraction of the cost of comparable airto-air units fabricated by conventional techniques.

Conclusions

This paper describes a design procedure by which superplastic materials, of complex shape but economical to manufacture, can be applied in heat transfer technology. There are, of course, many surface designs and possible applications that are not mentioned above, but a designer familiar with the forming process and the methods discussed in this paper will have available a design tool which could, in many applications, lead to very significant cost savings and performance improvement.

In general, the practical use of superplasticity is just beginning in heat transfer. The key to such use in the future lies in the development of designs and design approaches that can apply the unique properties of superplastic material to economic as well as technical advantage.

Acknowledgments

The authors must acknowledge the many people within the IBM Corporation who have been involved in the development of superplastic technology from its infancy; we are grateful particularly to R. C. Kay, without whose interest and material support this effort would not have been possible.

References

- 1. W. M. Kays and A. L. London, Compact Heat Exchangers, McGraw Hill Book Company, Inc., New York 1964.
- 2. W. M. Kays and A. L. London, "Heat-Transfer and Flow-Friction Characteristics of Some Compact Heat-Exchanger Surfaces, Part I-Test System and Procedure," Trans. ASME 72, 1075 (1950).
- 3. A. L. London and C. K. Ferguson, "Test Results of High-Performance Heat-Exchanger Surfaces Used in Aircraft Intercoolers and Their Significance for Gas-Turbine Regenerator Design," Trans. ASME 71, 17 (1949).
- 4. E. E. Underwood, "A Review of Superplasticity," J. Metals 14, 914 (1962).

- 5. W. A. Backofen, I. R. Turner and D. H. Avery, "Superplasticity in an Al-Zn Alloy," Trans. Am. Soc. Metals 57, 980 (1964).
- 6. P. Chaudhari, "Superplasticity," Science and Technology,
- September 1968, p. 42.

 7. D. S. Fields, Jr., "Sheet Thermoforming of a Superplastic Alloy," IBM J. Res. Develop. 9, 134 (1965).
- J. F. Hubert and R. C. Kay, "A Survey of Applications of Superplastic Metal Forming," Proc. 1971 Design Engineering Conference, ASME, New York, April 1971.
- 9. D. W. Davis, "Design Applications of Superplastic Alloys," Proc. 1971 Design Engineering Conference, ASME, New York, April 1971.
- 10. M. Jakob, Heat Transfer, Vol. 2, John Wiley and Sons, New York 1957, p. 202.
- 11. R. A. Bowman, A. C. Mueller and W. M. Nagle, "Mean Temperature Difference in Design," Trans. ASME 62, 288 (1940).
- 12. J. L. Mason, "Heat Transfer in Cross-flow," Proc. Appl. Mechanics, 2nd U.S. National Congress, 1954, p. 801.
- 13. W. M. Kays, Convective Heat and Mass Transfer, Mc-Graw-Hill Book Company, Inc., New York 1966, Ch. 12.

Received July 22, 1971

The authors are located at the IBM General Systems Division Laboratory, Rochester, Minnesota 55901.